Biosensors and Bioelectronics 24 (2009) 2417–2422

Contents lists available at ScienceDirect

Biosensors and Bioelectronics

journal homepage: www.elsevier.com/locate/bios

An ionic liquid supported CeO_2 nanoshuttles–carbon nanotubes composite as a platform for impedance DNA hybridization sensing

Wei Zhang[a], Tao Yang[a], Xuming Zhuang[a], Zhiyan Guo[b], Kui Jiao[a,*]

[a] Key Laboratory of Eco-chemical Engineering (Ministry of Education), College of Chemistry and Molecular Engineering, Qingdao University of Science and Technology, Qingdao 266042, China
[b] New Materials & Function Coordination Chemistry Laboratory, Qingdao University of Science and Technology, Qingdao 266042, China

ARTICLE INFO

Article history:
Received 17 October 2008
Received in revised form 3 December 2008
Accepted 12 December 2008
Available online 25 December 2008

Keywords:
CeO_2
Single-walled carbon nanotubes
Ionic liquid
DNA electrochemical biosensor
Electrochemical impedance spectroscopy
PEPCase gene

ABSTRACT

A novel nanocomposite membrane, comprising of nanosized shuttle-shaped cerium oxide (CeO_2), single-walled carbon nanotubes (SWNTs) and hydrophobic room temperature ionic liquid (RTIL) 1-butyl-3-methylimidazolium hexafluorophosphate ($BMIMPF_6$), was developed on the glassy carbon electrode (GCE) for electrochemical sensing of the immobilization and hybridization of DNA. The properties of the CeO_2–SWNTs–$BMIMPF_6$/GCE, the characteristics of the immobilization and hybridization of DNA were studied by cyclic voltammetry and electrochemical impedance spectroscopy (EIS) using $[Fe(CN)_6]^{3-/4-}$ as the redox indicator. The synergistic effect of nano-CeO_2, SWNTs and RTIL could dramatically enhance the sensitivity of DNA hybridization recognition. The electron transfer resistance (R_{et}) of the electrode surface increased after the immobilization of probe ssDNA on the CeO_2–SWNTs–$BMIMPF_6$ membrane and rose further after the hybridization of the probe ssDNA with its complementary sequence. The remarkable difference between the R_{et} value at the probe DNA-immobilized electrode and that at the hybridized electrode could be used for label-free EIS detection of the target DNA. The sequence-specific DNA of phosphoenolpyruvate carboxylase (PEPCase) gene from transgenically modified rape was detected by this DNA electrochemical biosensor. Under optimal conditions, the dynamic range for detecting the sequence-specific DNA of the PEPCase gene was from 1.0×10^{-12} mol/L to 1.0×10^{-7} mol/L, and the detection limit was 2.3×10^{-13} mol/L, suggesting that the CeO_2–SWNTs–$BMIMPF_6$ nanocomposite hold great promises for the applications in sensitive electrochemical biosensor.

1. Introduction

With the development of the products of transgenic plants, considerable interest has been focused on fast, simple and inexpensive methods for specific transgenic sequences detection. As compared with other analytical techniques, DNA electrochemical biosensor is widely used owing to its high sensitivity, simplicity and low cost (Qi et al., 2007; Li et al., 2007, 2008; Flechsig and Reske, 2007; Gonzalez et al., 2008). The immobilization of ssDNA probe on different types of transducer surfaces is the most critical step for fabrication of DNA biosensors to obtain low detection limit, high sensitivity, stability and selectivity (Arora et al., 2007; Sassolas et al., 2008).

Room temperature ionic liquid (RTIL), composed of organic cations and various anions, represents a kind of novel nonaqueous but polar solvent (Welton, 1999). It exhibits many unique advantages such as high chemical and thermal stabilities, negligible vapor pressure, high ionic conductivity, wide electrochemical windows, low toxicity and ability to dissolve a wide range of organic and inorganic compounds (Zhao et al., 2004). Therefore, it has great potential application in extraction and separation, organic synthesis, solar cell and so on (Fan et al., 2008; Ahmad and Singh, 2008; Chen et al., 2007). Recently, attempts to use ionic liquid in electrochemical analysis can be noted (Zhang and Zheng, 2008; Lu et al., 2006; Pauliukaite et al., 2008; Musameh and Wang, 2008). For example, Zhang et al. explored a novel biocomposite film based on ionic liquid and hyaluronic acid as an excellent platform for realizing direct electrochemistry and electrocatalysis of myoglobin (Zhang and Zheng, 2008). Increasing attention has been paid to the modified electrodes with ionic liquid and nanomaterial composite in hopes of combining their unique properties (Liu et al., 2007; Xiang et al., 2008; Maleki et al., 2008; Xiao et al., 2008). For instance, Liu et al. reported a laccase biosensor based on carbon nanotubes-ionic liquid gel film cast on hydrophobic graphite electrode surface (Liu et al., 2007). Xiang et al. studied the direct electron transfer of cytochrome c immobilized on gold nanoparticles/ionic liquid/carbon nanotubes nanohybrid film prepared by layer-by-layer self-assembly technique (Xiang et al., 2008). An ionic liquid doped DNA network was utilized to fabricate a novel

* Corresponding author. Tel.: +86 532 84022665; fax: +86 532 84023927.
E-mail address: kjiao@qust.edu.cn (K. Jiao).

0956-5663/$ – see front matter © 2008 Elsevier B.V. All rights reserved.
doi:10.1016/j.bios.2008.12.024

electrochemical H_2O_2 biosensor by embedding horseradish peroxide in the network (Guo et al., 2007). When RTIL was doped in DNA, the films obtained had good ionic conductivity (Nishimura et al., 2005). However, to our best knowledge, the application of ionic liquid combining with nanomaterials for the hybridization detection of DNA has not been reported.

In recent years, that inorganic oxide nanoparticles are utilized to be the immobilizing carriers of ssDNA probe is becoming the focus of research due to unique properties derived from their low dimensionality and possible quantum-confinement effects (Yang et al., 2007; Ma et al., 2008; Feng et al., 2006). Among the inorganic oxide nanoparticles, cerium oxide (CeO_2) has been exploited as a promising material for biosensing (Wei et al., 2006; Ansari et al., 2008) owing to its unusual properties including large surface area, excellent biocompatibility, nontoxicity, high chemical stability and strong adsorption ability (high isoelectric point ~9.2). It may be noted that positively charged surface of CeO_2 nanoparticles could be utilized for binding of negatively charged biomolecules. For instance, Ansari et al. developed a cholesterol biosensor by immobilizing cholesterol oxidase on sol–gel derived nano-structured CeO_2 film without any mediator (Ansari et al., 2008). A nanoporous CeO_2/chitosan composite was used for immobilization of ssDNA probe and detection of cancer gene (Feng et al., 2006). Despite of some advantages, the relatively poor conductivity of chitosan (Lu et al., 2006) confined the enhancement of the sensitivity of this biosensor.

In the present paper, RTIL 1-butyl-3-methylimidazolium hexafluorophosphate ($BMIMPF_6$) with high conductivity was introduced into a novel membrane comprising of nanosized CeO_2 and single-walled carbon nanotubes (SWNTs). The obtained CeO_2–SWNTs–$BMIMPF_6$ nanocomposite membrane integrated the strong adsorption ability of nano-CeO_2 to the DNA probes with the high ionic conductivity of RTIL, and the large surface area and excellent electron-transfer ability of SWNTs. The synergistic effect of this nanocomposite matrix could greatly enhance the loading of ssDNA probes and hence markedly improve the sensitivity of target DNA detection. The sequence-specific DNA of phosphoenolpyruvate carboxylase (PEPCase) gene from transgenically modified rape was satisfactorily detected by this DNA biosensor with label-free electrochemical impedance spectroscopic (EIS) method. Such a novel membrane may be used as a potential sensing platform for detection of other biomolecules.

2. Experimental

2.1. Apparatus and reagents

A CHI 660C electrochemical analyzer (Shanghai CH Instrument Company, Shanghai, China), which was in connection with a glassy carbon modified working electrode (diameter = 3 mm), a saturated calomel reference electrode (SCE) and a platinum wire counter electrode, was used for electrochemical measurements. The pH values of all solutions were measured by a model pHS-25 digital acidimeter (Shanghai Leici Factory, Shanghai, China). Scanning electron microscopy (SEM) was carried out using a JSM-6700F machine (JEOL, Tokyo, Japan).

Nanosized CeO_2 was synthesized as reported previously (Guo et al., 2008). Hydrophobic ionic liquid $BMIMPF_6$ was purchased from Hangzhou Kemer Chemical Co., Ltd. (Hangzhou, China). SWNTs were obtained from Shenzhen Nanotech. Port Co., Ltd. (Shenzhen, China). Sodium dodecylsulfate (SDS) and methylene blue (MB) were purchased from Shanghai Reagent Company (Shanghai, China) and used as received. Potassium ferricyanide ($K_3[Fe(CN)_6]$) and potassium ferrocyanide ($K_4[Fe(CN)_6]$) were purchased from Shanghai No. 1 Reagent Factory (Shanghai, China) and Shanghai Heng Da Chemical Co., Ltd. (Shanghai, China), respectively. All the chemicals are of analytical grade and solutions were prepared with Aquapro ultrapure water (Chongqing, China).

Materials for detection of PEPCase gene sequences: the 20-base oligonucleotides probe (ssDNA), its complementary DNA sequence (cDNA, target DNA, namely a 20-base fragment of PEPCase gene sequence, which was selected according to the transgenic sequence of phosphoenolpyruvate carboxylase gene in transgenically modified rape), single-base mismatched DNA sequence, double-base mismatched sequence and noncomplementary DNA sequence (ncDNA) were synthesized by Beijing SBS Gene Technology Co., Ltd. (Beijing, China). Their base sequences are listed below:

probe DNA (ssDNA): 5′-CAG CAC CTA GGC ATA GGT TC-3′;
target DNA (cDNA): 5′-GAA CCT ATG CCT AGG TGC TG-3′;
single-base mismatched DNA: 5′-GAA CCT ATG CCT AGG TG<u>G</u> TG-3′;
double-base mismatched DNA: 5′-GAA CCT <u>C</u>TG CCT AGG TG<u>G</u> TG-3′;
ncDNA: 5′-TGC GAT AAA GGA AAG GCT AT-3′.

All oligonucleotides stock solutions of 20-base oligomers (1.0×10^{-6} mol/L) were prepared with Tris–HCl buffer (5.0 mmol/L Tris–HCl, 50.0 mmol/L NaCl, pH 7.0), and stored at 4 °C. More diluted solutions were obtained via diluting aliquot of the stock solution with ultrapure water prior to use. The hybridization solution was diluted with 2× SSC (pH 7.5), which consists of 0.30 mol/L NaCl and 0.03 mol/L sodium citrate tribasic dihydrate ($C_6H_5Na_3O_7 \cdot 2H_2O$).

2.2. Preparation of the CeO_2–SWNTs–$BMIMPF_6$/GCE

The SWNTs were purified through refluxing in HNO_3–H_2SO_4 (v/v, 1:1) mixture for 2 h at 55 °C and then for 3 h at 80 °C, washing with ultrapure water, and dried under vacuum. 10 mg of purified SWNTs were dispersed in 10 mL of dimethylformamide (DMF) with the aid of ultrasonication for 2 h to give a 1.0 mg/mL homogeneous black suspension. Then 2 mg of CeO_2 nanoshuttles were added to the SWNTs suspension and the resulted suspension was ultrasonicated for 2 h. After that, $BMIMPF_6$ (final concentration (v/v) 3.0%) was dispersed in the CeO_2–SWNTs composite with the aid of ultrasonication (Xiao et al., 2007). Finally, a uniform CeO_2–SWNTs–$BMIMPF_6$ nanocomposite suspension was obtained.

Before modification, the GCE was freshly polished prior to each experiment with 0.3 μm and 0.05 μm α-Al_2O_3 paste, respectively, and rinsed with ultrapure water after each polishing step, finally cleaned ultrasonically in ethanol and water, respectively, for 3 min. 10 μL of the CeO_2–SWNTs–$BMIMPF_6$ suspension was dropped on the GCE and let it dry at room temperature for 2 h, thus a uniform membrane coated electrode (CeO_2–SWNTs–$BMIMPF_6$/GCE) was obtained. The CeO_2/GCE, CeO_2–$BMIMPF_6$/GCE and CeO_2–SWNTs/GCE were fabricated through similar procedure.

2.3. DNA probe immobilization and hybridization

Immobilization of ssDNA probes was performed by immersing the CeO_2–SWNTs–$BMIMPF_6$/GCE into 2.0 mL Tris–HCl buffer (pH 7.0) solution containing 1.0×10^{-6} mol/L ssDNA probes for 2 h at room temperature, followed by washing the electrode with 0.5% SDS solution and then rinsing it with ultrapure water to remove the unimmobilized ssDNA, and this probe-captured electrode was denoted as ssDNA/CeO_2–SWNTs–$BMIMPF_6$/GCE.

The ssDNA/CeO_2–SWNTs–$BMIMPF_6$/GCE was immersed into a hybridization solution (2× SSC buffer, pH 7.5) containing the target DNA and hybridized at 0.4 V for 500 s, followed by washing the electrode with 0.5% SDS to remove the unhybridized DNA, and this hybridization modified electrode was denoted as dsDNA/

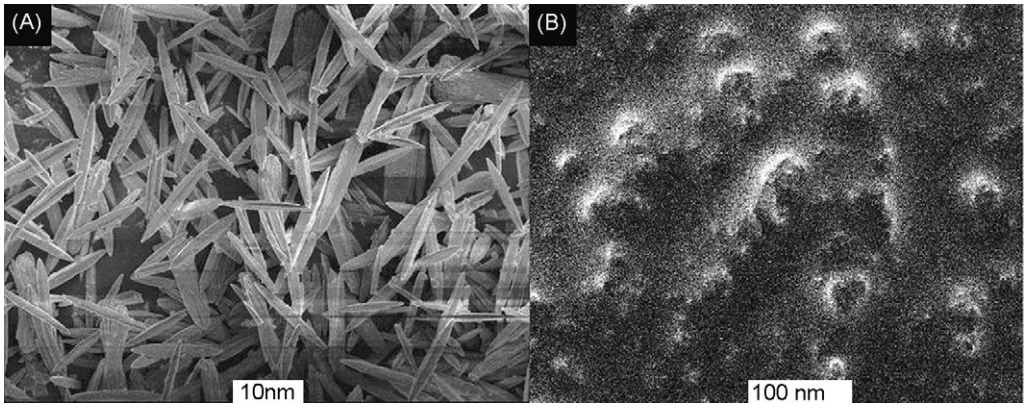

Fig. 1. SEM images of the synthesized CeO_2 (A) and CeO_2–SWNTs–$BMIMPF_6$ nanocomposite membrane (B).

CeO_2–SWNTs–$BMIMPF_6$/GCE. The hybridizations of probe ssDNA with single-base mismatched DNA, double-base mismatched DNA and ncDNA were carried out through similar procedure.

2.4. Electrochemical measurements

Cyclic voltammetric (CV) measurements of 5.0 mmol/L $K_3Fe(CN)_6$ and 5.0 mmol/L $K_4Fe(CN)_6$ were performed with 0.1 mol/L KCl as the supporting electrolyte. The scan rate was 100 mV/s.

EIS measurements were also carried out in 5.0 mmol/L $[Fe(CN)_6]^{3-/4-}$ (1:1) containing 0.1 mol/L KCl. The AC voltage amplitude was 5 mV and the voltage frequencies ranged from 10 kHz to 0.05 Hz. The applied potential was 0.172 V.

The reported result for every electrode in this paper was the mean value of three parallel measurements.

3. Results and discussion

3.1. Morphology of the synthesized CeO_2 and CeO_2–SWNTs–$BMIMPF_6$ nanocomposite membrane

The morphology of synthesized CeO_2 was characterized by SEM as shown in Fig. 1A. It can be seen that the products consist of homogeneous and intact shuttle-shaped nano-CeO_2. The CeO_2–SWNTs–$BMIMPF_6$ nanocomposite can form a membrane on the surface of GCE and its SEM image is displayed in Fig. 1B. The CeO_2 nanoshuttles and SWNTs were uniformly dispersed in RTIL, which provided an enhanced loading membrane for immobilization of ssDNA probes.

3.2. Electrochemical characteristics of the CeO_2–SWNTs–$BMIMPF_6$ nanocomposite membrane

The cyclic voltammograms of 5.0 mmol/L $[Fe(CN)_6]^{3-/4-}$ at the CeO_2/GCE (a), CeO_2–$BMIMPF_6$/GCE (b), CeO_2–SWNTs/GCE (c) and CeO_2–SWNTs–$BMIMPF_6$/GCE (d) are shown in Fig. 2A. The peak current (i_p) of $[Fe(CN)_6]^{3-/4-}$ increased and the peak-to-peak separation (ΔE_p) decreased in the order of CeO_2/GCE (a), CeO_2–$BMIMPF_6$/GCE (b), CeO_2–SWNTs/GCE (c) and CeO_2–SWNTs–$BMIMPF_6$/GCE (d). A couple of well-defined peaks were observed for the CeO_2–SWNTs–$BMIMPF_6$/GCE. The ΔE_p was 0.097 V, and the peak currents of cathodic and anodic peaks were near equal, indicating that the electrochemical process was quasi-reversible. The i_p changed linearly with the square root of the scan rate ($\nu^{1/2}$) in the range studied (50–500 mV/s), meaning that the electrochemical process was controlled by diffusion.

The microscopic electroactive areas of the modified GCEs were obtained by CV using 5.0 mmol/L $[Fe(CN)_6]^{3-/4-}$ as the redox probe at different scan rates according to the Randles–Sevčik equation (Gao et al., 2006; Rezaei and Zare, 2008): $i_{pa} = 2.69 \times 10^5 AD^{1/2} n^{3/2} \nu^{1/2} C$. Where i_{pa} refers to the anodic peak current, n the electron transfer number, A the surface area of the electrode, D the diffusion coefficient, C the concentration of $[Fe(CN)_6]^{3-/4-}$ and ν the scan rate. For 5.0 mmol/L $[Fe(CN)_6]^{3-/4-}$ in 0.1 mol/L KCl electrolyte, $n = 1$, $D = 6.70 \times 10^{-6}$ cm^2/s, then from the slope of the i_{pa}–$\nu^{1/2}$ relation, the microscopic area can be calculated. The average value of the active surface area (average of three measurements) for the CeO_2–SWNTs–$BMIMPF_6$/GCE was 0.32 cm^2 compared to 0.25 cm^2 for the CeO_2–SWNTs/GCE, 0.13 cm^2 for the CeO_2–$BMIMPF_6$/GCE and 0.05 cm^2 for the CeO_2/GCE. Herein, the synergistic effect of

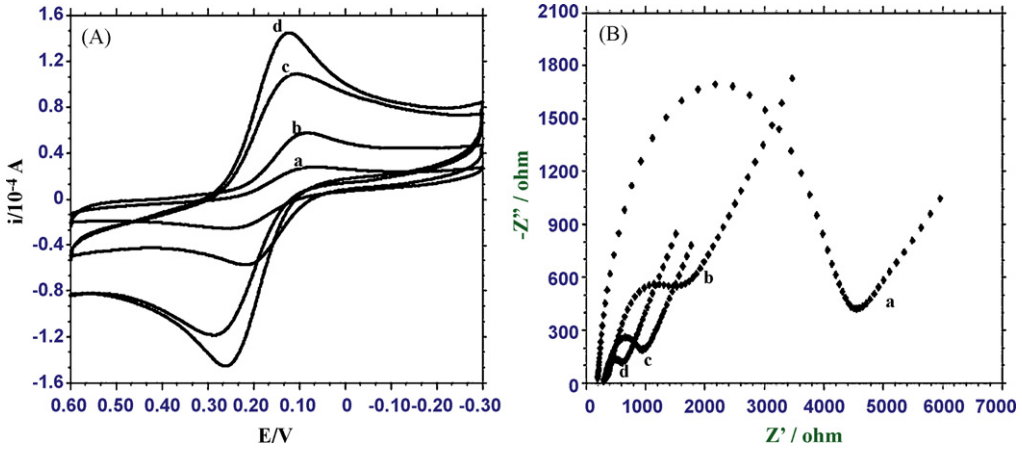

Fig. 2. Cyclic voltammograms (A) and Nyquist diagrams (B) of 5.0 mmol/L $[Fe(CN)_6]^{3-/4-}$ in 0.1 mol/L KCl recorded at (a) CeO_2/GCE, (b) CeO_2–$BMIMPF_6$/GCE, (c) CeO_2–SWNTs/GCE and (d) CeO_2–SWNTs–$BMIMPF_6$/GCE.

nano-CeO_2, SWNTs and RTIL on enhancing the electroactive surface area was outstanding.

EIS was carried out to probe the interfacial electron-transfer resistance (R_{et}) at the modified electrode (Suni, 2008). Generally, the semicircle portion observed at high frequencies in the Nyquist diagrams corresponds to the electron-transfer limiting process. The R_{et} value can be directly measured as the semicircle diameter. The Nyquist diagrams of different modified electrodes in 5.0 mmol/L $[Fe(CN)_6]^{3-/4-}$ containing 0.1 mol/L KCl are shown in Fig. 2B. The R_{et} value for the CeO_2/GCE (a) was estimated to be $4.652 \times 10^3\ \Omega$. As compared with curve a, the R_{et} value ($1.516 \times 10^3\ \Omega$) decreased dramatically at the CeO_2–BMIMPF$_6$/GCE (b), which could be ascribed to the high ionic conductivity of ionic liquid. For the CeO_2–SWNTs/GCE (c), the R_{et} value ($0.723 \times 10^3\ \Omega$) decreased further, indicating that SWNTs form high electron conduction pathways between the electrode and electroactive indicator. In particular, for the CeO_2–SWNTs–BMIMPF$_6$/GCE (d), simultaneous introduction of ionic liquid and SWNTs into the nanocomposite membrane reduced the R_{et} value ($0.405 \times 10^3\ \Omega$) to the minimum, which revealed the existence of synergistic effect in the membrane, and the synergistic effect might be due to the high ionic conductivity of ionic liquid and the large surface area of CeO_2, and the large surface area and excellent electron-transfer ability of SWNTs.

3.3. Influence of BMIMPF$_6$ on the nanocomposite membrane

The influence of ionic liquid BMIMPF$_6$ on the CeO_2–SWNTs–BMIMPF$_6$ nanocomposite membrane was studied. As reported previously, ionic liquid could interact with carbon nanotubes through 'π–π' interaction, which made the compactly entangled SWNTs bundles form much finer bundles (Fukushima et al., 2003). Thus, the electrocatalytical property of SWNTs can be significantly improved. The ionic liquid BMIMPF$_6$ may also act as an efficient binder (Musameh et al., 2008) to connect nano-CeO_2 and SWNTs, which made the nanocomposite membrane more uniform.

The ratio of BMIMPF$_6$ in the nanocomposite membrane had a pronounced effect on the performance of the CeO_2–SWNTs–BMIMPF$_6$/GCE. The CV peak currents of $[Fe(CN)_6]^{3-/4-}$ increased with enhancing the volume ratio of BMIMPF$_6$ in the CeO_2–SWNTs–BMIMPF$_6$ suspension. However, when its amount was too much, it would block the electron transfer as it might form a thick membrane on the surface of nano-CeO_2 and SWNTs. When it exceeded 3.0% the peak currents tended to stable. The background current also varied with the amount of BMIMPF$_6$, and when it was about 3.0% the signal-to-background ratio was the largest. Therefore, the ratio of BMIMPF$_6$ was fixed at 3.0% in this work.

3.4. Electrochemical studies on DNA immobilization and hybridization

Fig. 3 shows the Nyquist diagrams of 5.0 mmol/L $[Fe(CN)_6]^{3-/4-}$ at the CeO_2–SWNTs–BMIMPF$_6$/GCE (a), ssDNA/CeO_2–SWNTs–BMIMPF$_6$/GCE (b) and the hybridized dsDNA/CeO_2–SWNTs–BMIMPF$_6$/GCE (c), respectively. After the ssDNA probes were immobilized on the CeO_2–SWNTs–BMIMPF$_6$/GCE, the negatively charged phosphate backbone of probe ssDNA prevented $[Fe(CN)_6]^{3-/4-}$ from reaching the electrode surface during the redox process, and therefore led to a larger R_{et} value (curve b) than that at the CeO_2–SWNTs–BMIMPF$_6$/GCE (curve a). When the probe DNA was hybridized with its complementary target DNA (cDNA) in solution, the R_{et} value increased greatly to a much larger value (curve c). After hybridization, the negative charges on the electrode surface increased remarkably and the surface membranes became thicker, which might raise the R_{et} value. Therefore, from the changes of the R_{et} value, the immobilization and hybridization of DNA on this CeO_2–SWNTs–BMIMPF$_6$/GCE platform could be understood clearly.

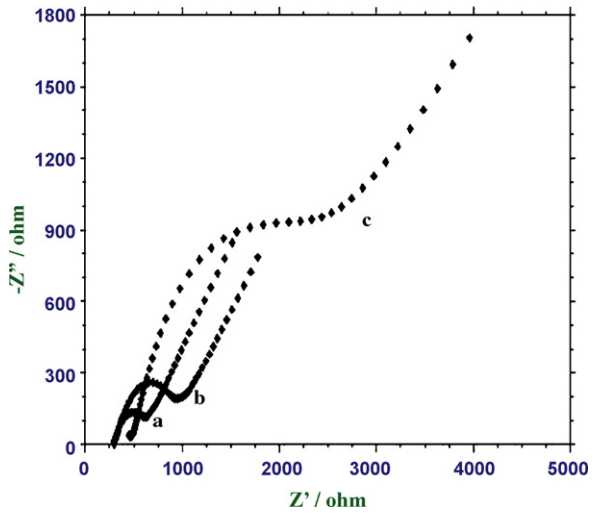

Fig. 3. Nyquist diagrams recorded at (a) CeO_2–SWNTs–BMIMPF$_6$/GCE, (b) probe ssDNA/CeO_2–SWNTs–BMIMPF$_6$/GCE and (c) dsDNA/CeO_2–SWNTs–BMIMPF$_6$/GCE. Supporting electrolyte solution was 5.0 mmol/L $[Fe(CN)_6]^{3-/4-}$ containing 0.1 mol/L KCl.

The stability of oligonucleotide probes on the modified electrode surface is believed to be a key factor to achieve high sensitivity. To investigate the stability of the ssDNA/CeO_2–SWNTs–BMIMPF$_6$/GCE, the electrode was incubated in B-R buffer solution (pH 6.0), Tris–HCl buffer solution (pH 7.0) and 2× SSC solution (pH 7.5) at 30 °C for 10 h, respectively. Then the probe DNA modified electrode was tested in 5.0 mmol/L $[Fe(CN)_6]^{3-/4-}$ containing 0.1 mol/L KCl. The magnitudes of all the obtained EIS signals were almost unchanged. Meanwhile, the UV–vis spectra of all the incubation solutions were recorded, respectively, and no DNA absorption peaks at 260 nm were observed. The solutions for baseline correction were unincubated solutions, respectively. The experiments suggested that the DNA probe would not eluted from the surface of the modified electrode. The results demonstrated that the probe ssDNA/CeO_2–SWNTs–BMIMPF$_6$/GCE had high stability and can be applied to the detection of target DNA sequence.

DNA immobilization time, hybridization potential and hybridization time were optimized via EIS measurements. The ssDNA probe was immobilized by immersing the CeO_2–SWNTs–BMIMPF$_6$/GCE into a 2 mL 1.0×10^{-6} mol/L DNA probe of Tris–HCl buffer solution (pH 7.0) for different time at room temperature, and the Nyquist diagrams at the electrode after every immobilization of the probe DNA were respectively recorded. The results showed that the R_{et} value at the probe-modified electrode rose gradually at first (up to 2 h) and then reached a constant level beyond 2 h. Therefore, an adsorption time of 2 h was selected for the immobilization of probe DNA in our experiments. The probe DNA on the membrane was hybridized with cDNA at different constant potentials, such as 0.2, 0.3, 0.4, 0.5, 0.6 and 0.7 V, and the Nyquist diagrams at the electrode before and after hybridization of the probe DNA were respectively recorded. The R_{et} difference value after and before hybridization of the probe DNA (ΔR_{et}) was evaluated. The larger the ΔR_{et} value, the better the hybridization. The largest ΔR_{et} value was obtained when the hybridization was conducted at 0.4 V. Thus, the optimal hybridization potential was selected as 0.4 V. The probe DNA was hybridized with cDNA at 0.4 V for from 100 s to 700 s. The results showed that the ΔR_{et} value rose with the increase of the hybridization time from 100 s to 500 s and then reached a constant level beyond 500 s. A hybridization time of 500 s was used in our experiments.

According to the method reported (Yang et al., 2008), the surface densities of the ssDNA probes on different modified electrodes were evaluated. The brief principle of this method is firstly to

calculate the mol quantity of methylene blue (MB) from the cyclic voltammetry, based on following equation: $N = Q/(neN_A)$, where N represents the mol quantity of MB; Q the electric charge quantity of MB reduction process; n the number of electrons participating in the reaction, $n = 2$ in this experiment; e the electric charge quantity of one electron, which is 1.6×10^{-19} C; N_A represents Avogadro's number, and its value is 6.02×10^{23} mol^{-1}. In this experiment, the reaction of MB at the probe-modified electrode surface is a surface-controlled process, and we obtained the electric charge quantity of MB from the cyclic voltammogram of its reaction. Therefore, N was calculated to be 5.10×10^{-11} mol for the ssDNA/CeO_2/GCE, 1.03×10^{-10} mol for the ssDNA/CeO_2–BMIMPF$_6$/GCE, 1.53×10^{-10} mol for the ssDNA/CeO_2–SWNTs/GCE and 1.90×10^{-10} mol for the ssDNA/CeO_2–SWNTs–BMIMPF$_6$/GCE, respectively. One MB molecule can be combined with one G base, and every PEPCase ssDNA probe sequence contains five G bases. Therefore, the surface density of the ssDNA probes was calculated as the product of the amount of MB and the stoichiometric ratio of MB to the ssDNA probe (5:1). The apparent area of every GCE (diameter = 3 mm) used in this experiment was 7.07×10^{-2} cm^2, and the surface density of the ssDNA probes on the CeO_2–SWNTs–BMIMPF$_6$/GCE was estimated to be 5.40×10^{-10} mol/cm^2, which was larger than that on the CeO_2/GCE (1.45×10^{-10} mol/cm^2), CeO_2–BMIMPF$_6$/GCE (2.93×10^{-10} mol/cm^2) and CeO_2–SWNTs/GCE (4.35×10^{-10} mol/cm^2). The results clarified that the synergistic effect of the CeO_2–SWNTs–BMIMPF$_6$ nanocomposite membrane could greatly enhance the loading of ssDNA probes on the electrode surface.

3.5. Selectivity, reproducibility and regeneration of DNA hybridization recognition

The selectivity of the sensor was investigated by measuring the responses of different DNA hybridization sequences related to PEPCase gene in transgenically modified rape. After hybridization of the DNA probe, the changes of the Nyquist diagram of $[Fe(CN)_6]^{3-/4-}$ are shown in Fig. 4. The curve a is the Nyquist diagram at the probe ssDNA/CeO_2–SWNTs–BMIMPF$_6$/GCE. After hybridization of the DNA probe with cDNA, the change of the Nyquist diagram is shown in curve b. The R_{et} value increased obviously, suggesting that hybrids (dsDNA) were formed at the electrode. The increase of the R_{et} value was negligible after the DNA probe was hybridized with the noncomplementary sequence (curve c), indicating that the hybridization reaction was not achieved. After the DNA probe was hybridized with the single-base mismatched sequence (curve d) or double-base mismatched sequence (curve e), the increase of the R_{et} value was much smaller than that obtained from the hybridization with cDNA (curve b). And the single-base mismatched sequence and double-base mismatched sequence could also be recognized via comparing the increase of the R_{et} value. The results demonstrated that this DNA biosensor displayed very high selectivity for the hybridization detection.

The reproducibility of any biosensor is extremely important to practical application. In our test, six parallel-made DNA biosensors were used to detect 1.0×10^{-10} mol/L target DNA and a relative standard deviation (R.S.D.) of 3.75% ($n = 6$) was estimated, showing the high reproducibility of this DNA electrochemical biosensor.

The regeneration ability of this impedance-based DNA biosensor was also evaluated. The dsDNA on the hybridized electrode was hot denatured by immersing the electrode into boiling water for 10 min, and then cooled down rapidly with an ice salt bath, followed by rinsing the electrode with ultrapure water. The Nyquist diagrams of 5.0 mmol/L $[Fe(CN)_6]^{3-/4-}$ at the regenerated probe modified electrode and its hybridized electrode were recorded. The results indicated that the two R_{et} values at the two electrodes and their ΔR_{et} value were almost the same as those obtained in the first experiment, respectively. Successive experiments showed that the DNA biosensor could be reproduced for three times without losing its sensitivity, indicating the fine regeneration ability of this DNA biosensor.

3.6. Detection of sequence-specific DNA of PEPCase gene

The difference between the R_{et} value (namely ΔR_{et}) of 5.0 mmol/L $[Fe(CN)_6]^{3-/4-}$ containing 0.1 mol/L KCl at the probe ssDNA/CeO_2–SWNTs–BMIMPF$_6$/GCE and that at the hybridization modified electrode (dsDNA/CeO_2–SWNTs–BMIMPF$_6$/GCE) was used to be the measurement signal to determine the PEPCase gene target sequence. The concentration of the PEPCase gene target sequence in the hybridization solution was changed from 1.0×10^{-7} mol/L to 1.0×10^{-12} mol/L, and the results are shown in Fig. 5. The ΔR_{et} value between before and after hybridization was linear with the logarithm of the PEPCase target sequence concentrations. The dynamic detection range for the sequence-specific

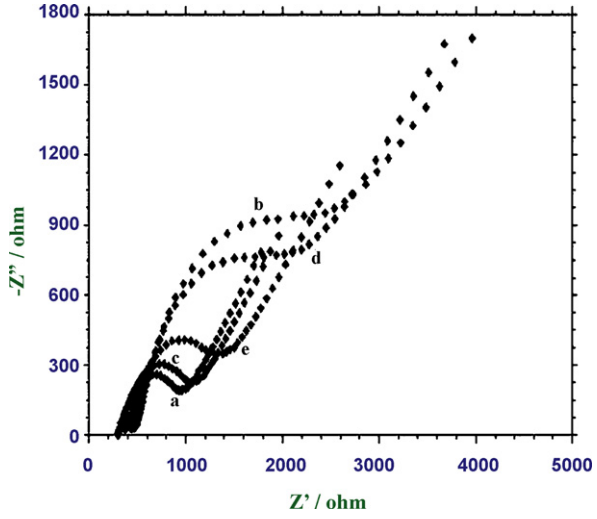

Fig. 4. Nyquist diagrams recorded at (a) ssDNA/CeO_2–SWNTs–BMIMPF$_6$/GCE, (b) dsDNA/CeO_2–SWNTs–BMIMPF$_6$/GCE (hybridization with cDNA), (c) the electrode hybridized with ncDNA, (d) the electrode hybridized with single-base mismatched DNA and (e) the electrode hybridized with double-base mismatched DNA. Conditions were the same as in Fig. 3.

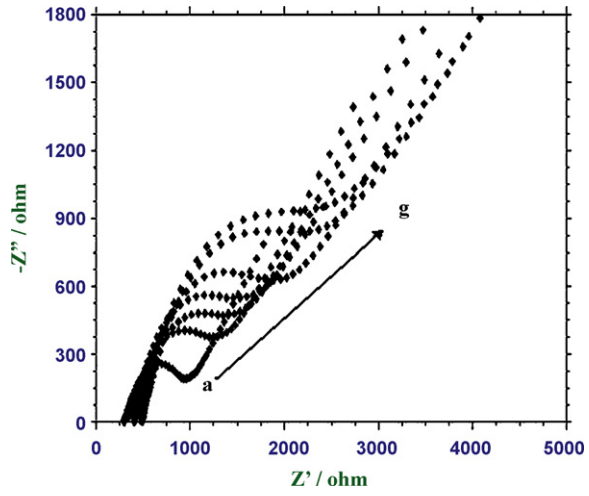

Fig. 5. Nyquist diagrams recorded at (a) ssDNA/CeO_2–SWNTs–BMIMPF$_6$/GCE and after hybridization reaction with different concentrations of sequence-specific DNA of PEPCase gene: (b) 1.0×10^{-12} mol/L, (c) 1.0×10^{-11} mol/L, (d) 1.0×10^{-10} mol/L, (e) 1.0×10^{-9} mol/L, (f) 1.0×10^{-8} mol/L and (g) 1.0×10^{-7} mol/L. Conditions were the same as in Fig. 3.

Table 1
Comparison of the performance of the proposed biosensor with that of some other nano-oxide-based DNA biosensors.

Method	This work	Yang et al. (2007)	Ma et al. (2008)	Feng et al. (2006)
Matrix for DNA immobilization	CeO_2–SWNTs–$BMIMPF_6$/GCE	MWNTs/ZrO_2/GCE	SiO_2/PATP/Au	CeO_2/CHIT/GCE
Detection method	EIS	DPV with daunomycin as indicator	EIS	DPV with MB as indicator
Detection limit (mol/L)	2.3×10^{-13}	7.5×10^{-11}	1.5×10^{-12}	1.0×10^{-11}
Detection range of target DNA (mol/L)	1.0×10^{-12}–1.0×10^{-7}	1.49×10^{-10}–9.32×10^{-8}	1.0×10^{-11}–1.0×10^{-6}	1.59×10^{-11}–1.16×10^{-7}

DNA of PEPCase gene was from 1.0×10^{-12} mol/L to 1.0×10^{-7} mol/L with the regression equation ΔR_{et} (Ω) = 5.285 lg C + 27.632 and the regression coefficient (R) 0.9952. The detection limit was 2.3×10^{-13} mol/L using 3σ, where σ was the relative standard deviation (R.S.D.) of eleven parallel measurements of the blank solution. The results demonstrated that the sensitivity of this impedance-based DNA biosensor was good enough for the PEPCase gene sequence detection.

The performance of the proposed biosensor was compared with that of some other DNA electrochemical biosensors based on nano-oxide, as listed in Table 1. It is apparent that the proposed DNA biosensor had a much lower detection limit and wider detection range for the target DNA assay than the other three.

4. Conclusions

In this paper, a CeO_2–SWNTs–$BMIMPF_6$ nanocomposite matrix was applied to the DNA hybridization sensing. The remarkable synergistic effect of this nanocomposite could greatly enhance the immobilization of the DNA probes and hence markedly improve the sensitivity of target DNA detection. The simple manipulation procedure, fast response, fine selectivity, high sensitivity and wide dynamic detection range are the main features of the proposed DNA biosensor. This is the first application of ionic liquid combining with nanomaterials to fabricate a DNA electrochemical hybridization biosensor.

Acknowledgments

This work was supported by the National Natural Science Foundation of China (No. 20635020, No. 20805025), Doctoral Foundation of the Ministry of Education of China (No. 20060426001) and Doctoral Fund of QUST (0022278).

References

Ahmad, S., Singh, S., 2008. Electrochem. Commun. 10, 895–898.
Ansari, A.A., Kaushik, A., Solanki, P.R., Malhotra, B.D., 2008. Electrochem. Commun. 10, 1246–1249.
Arora, K., Prabhakar, N., Chand, S., Malhotra, B.D., 2007. Biosens. Bioelectron. 23, 613–620.
Chen, D., Zhang, Q., Wang, G., Zhang, H., Li, J.H., 2007. Electrochem. Commun. 9, 2755–2759.
Fan, J., Fan, Y.C., Pei, Y.C., Wu, K., Wang, J.J., Fan, M.H., 2008. Sep. Purif. Technol. 61, 324–331.
Feng, K.J., Yang, Y.H., Wang, Z.J., Jiang, J.H., Shen, G.L., Yu, R.Q., 2006. Talanta 70, 561–565.
Flechsig, G.U., Reske, T., 2007. Anal. Chem. 79, 2125–2130.
Fukushima, T., Kosaka, A., Ishimura, Y., Yamamoto, T., Takigawa, T., Ishii, N., Aida, T., 2003. Science 300, 2072–2074.
Gao, X.H., Wei, W.Z., Yang, L., Guo, M.L., 2006. Electroanalysis 18, 485–492.
Gonzalez, M.D., Muniz, A.E., Garcia, M.B.G., Garcia, A.C., 2008. Biosens. Bioelectron. 23, 1340–1346.
Guo, C.L., Song, Y.H., Wei, H., Li, P.C., Wang, L., Sun, L.L., Sun, Y.J., Li, Z., 2007. Anal. Bioanal. Chem. 389, 527–532.
Guo, Z.Y., Du, F.L., Li, G.C., Cui, Z.L., 2008. Cryst. Growth. Des. 8, 2674–2677.
Li, X.M., Ju, H.Q., Du, L.P., Zhang, S.S., 2007. J. Inorg. Biochem. 101, 1165–1171.
Li, X.M., Xia, J.P., Zhang, S.S., 2008. Anal. Chim. Acta 622, 104–110.
Liu, Y., Huang, L.J., Dong, S.J., 2007. Biosens. Bioelectron. 23, 35–41.
Lu, X.B., Hu, J.Q., Yao, X., Wang, Z.P., Li, J.H., 2006. Biomacromolecules 7, 975–980.
Ma, Y., Jiao, K., Yang, T., Sun, D.X., 2008. Sens. Actuators B 131, 565–571.
Maleki, N., Safavi, A., Farjami, E., Tajabadi, F., 2008. Anal. Chim. Acta 611, 151–155.
Musameh, M., Wang, J., 2008. Anal. Chim. Acta 606, 45–49.
Musameh, M.M., Kachoosangi, R.T., Compton, R.G., 2008. Analyst 133, 133–138.
Nishimura, N., Nomura, Y., Nakamura, N., Ohno, H., 2005. Biomaterials 26, 5558–5563.
Pauliukaite, R., Doherty, A.P., Murnaghan, K.D., Brett, C.M.A., 2008. Electroanalysis 20, 485–490.
Qi, H.L., Li, X.X., Chen, P., Zhang, C.X., 2007. Talanta 72, 1030–1035.
Rezaei, B., Zare, S.Z.M., 2008. Sens. Actuators B 134 (2008), 292–299.
Sassolas, A., Bouvier, B.D.L., Blum, L.J., 2008. Chem. Rev. 108, 109–139.
Suni, I.I., 2008. Trends Anal. Chem. 27, 604–611.
Wei, Y., Li, M.G., Jiao, S.F., Huang, Q.N., Wang, G.F., Fang, B., 2006. Electrochim. Acta 52, 766–772.
Welton, T., 1999. Chem. Rev. 99, 2071–2083.
Xiang, C.L., Zou, Y.J., Sun, L.X., Xu, F., 2008. Electrochem. Commun. 10, 38–41.
Xiao, F., Zhao, F.Q., Li, J.W., Liu, L.Q., Zeng, B.Z., 2008. Electrochim. Acta 53, 7781–7788.
Xiao, F., Zhao, F.Q., Li, J.W., Yan, R., Yu, J.J., Zeng, B.Z., 2007. Anal. Chim. Acta 596, 79–85.
Yang, T., Zhang, W., Du, M., Jiao, K., 2008. Talanta 75, 987–994.
Yang, Y.H., Wang, Z.J., Yang, M.H., Li, J.S., Zheng, F., Shen, G.L., Yu, R.Q., 2007. Anal. Chim. Acta 584, 268–274.
Zhang, Y., Zheng, J.B., 2008. Electrochem. Commun. 10, 1400–1403.
Zhao, F., Wu, X.E., Wang, M.K., Liu, Y., Gao, L.X., Dong, S.J., 2004. Anal. Chem. 76, 4960–4967.